SPEEDING UP MODEL CORRELATION WITH BREAKOUT MODELS: THE VIPER INTEGRATED THERMAL MODEL CORRELATION STORY

Lisa Erickson[1], Veronica Pizor[1], Thomas Slusser[1], Jodi Turk[2], Elijah Stewart[2], Chane Sladek[3], Cameron Moen[3], Blain Lancaster[3], Quoc Nguyen[3], Thomas Paul[3], Glenn Waguespack[3], Rich Hogen[3], Jose Dobarco-Otero[4]

NASA Johnson Space Center[1], NASA Marshall Space Flight Center[2], Amentum[3], HX5,LLC[4]

ABSTRACT

Correlated integrated thermal models (ITMs) of spacecraft are needed to verify that hardware will stay within their Allowable Flight Temperature (AFT) limits. Unfortunately, the model correlation process is slow. Large models with hundreds of sensors can take several months to correlate. To speed up this process, many have pursued developing and using algorithms that find an optimal set of specified model parameters that minimize error. However, these algorithms still require models to run for many iterations and cannot address model deviations due to missing contacts or oversimplified geometries. Additionally, past projects have used engineering judgment to divide up correlation activities between multiple analysts. However, the problem of 'how to split up the correlation activities' is challenging. The Volatiles Investigating Polar Exploration Rover (VIPER) thermal team was recently faced with this problem.

In this paper, we present *Veronica*, a new approach developed by the VIPER thermal team to speed up spacecraft ITM correlation by parallelizing the process as much as possible. *Veronica* leverages the fact that vehicles often have different thermal zones that are *mostly* independent of each other. The key to the *Veronica* approach is splitting up the ITM, according to a specific criterion, into many faster running "breakout models". By correlating these "breakout models" in parallel, the overall correlation effort can be sped up. Using *Veronica*, the VIPER thermal team was able to use 14 analysts to correlate the ITM within 22 weeks (spanning Thanksgiving, Christmas, and New Years). After only updating the VIPER ITM with changes used to correlate the "breakout models", we were able to achieve an overall Root Mean Square (RMS) error of 7.4C for hot thermal balance and 10C for cold thermal balance. Out of 37 total key components, 54% had RMS errors within 5C and 81% had errors within 10C.

INTRODUCTION

A spacecraft integrated thermal model (ITM) that is correlated to thermal vacuum (TVAC) data is essential for verification. It is not practical to verify that components will stay within Allowable Flight Temperature (AFT) limits via test. Therefore, it is standard practice use correlated models to verify that ATF limits will not be exceeded in flight [1] [2] [3].

During the correlation process, model parameters are methodically adjusted until the ITM's predictions match test data within an allowed error. Unfortunately, this process requires much iteration has a reputation for being slow, particularly when an ITM is large and when the iteration is performed manually [4, 5]. To speed up this process, a number of optimization algorithms been developed that can automatically search for a set of pre-specified parameters that minimizes error [6], [7] , [8] , [9], [10]. Several have been implemented into thermal modeling software [11] [5]

[12]. These algorithms have two main limitations (1) they often can accidently find local minimum – i.e. get stuck at a solution that does not have the lowest error [11], and (2) they cannot address model deviations due to incorrect heat dissipations, missing contacts, or oversimplified geometries. Also, to speed up model correlation, others have proposed to use reduced order models – which can run much faster [4]. This approach, as well as the combination of detailed and reduced order models can all save correlation time – but requires programs to invest in reduced order model development in advance.

Another way to speed up model correlation is to parallelize the process between multiple analysts. This is the approach that was taken by the Volatiles Investigating Polar Exploration Rover (VIPER) thermal team. Past NASA projects have used engineering judgment to divide up correlation activities between multiple analysts. However, to the best of our knowledge, there is no public work on how to split up correlation activities. The "Thermal Testing" chapter of the *Spacecraft Thermal Control Handbook* implies that analysts could split work up by thermal zones, but changes made to one heat transfer path could impact another [1]. Guidance is given to first attempt to correlate thermal zones with largest temperature discrepancies [1].

The VIPER thermal team saw a need to parallelize the correlation approach for several reasons. First, they were given a hard deadline of 22 weeks - spanning Thanksgiving and New Years to correlate the VIPER ITM. However, prior to TVAC, the ITM ran slow. It took about 10 minutes to run a steady state hot thermal balance case and 40 minutes to run a steady state cold thermal balance case. There was not a reduced order ITM available. Second, a minimum of 141 sensors needed to be correlated and the model had over 1300 contacts between nodes/surfaces (excluding the test enclosure). Third, at the start of TVAC, the VIPER ITM was still undergoing updates to improve its fidelity and the thermal radiant heat enclosure (TRHE) [13] was not yet correlated. Lastly, up to 14 analysts were available to help with the correlation process.

To correlate the VIPER ITM, we developed *Veronica*, an approach that helps speed up spacecraft ITM correlation by enabling the majority of correlation steps to be carried out by multiple analysts in parallel. To create *Veronica*, we made two observations: (1) vehicle's typically have different 'thermal zones' that are mostly independent of each other [1], and (2) if component A is not a major contributor to component B's thermal balance, then the accuracy of A's temperature is not that important when predicting the temperature of B. We demonstrate this observation with an example in section "BACKGROUND: Observations Behind *Veronica*". According to these observations, if we correlate components within one a thermal zone, there should be negligible to acceptably small impacts to other thermal zones.

The key idea behind *Veronica* is that it is possible to split up an ITM into many smaller 'breakout models' that can match the full model's predictions, within a small error, that can just be used for correlating components within a particular thermal zone. A breakout model for one thermal zone, may exclude and/or not attempt to correlate components outside it. One challenge we faced when creating *Veronica* is determining the criteria for including/excluding components from breakout models. We present criteria for what to include/exclude in section "DESIGN: Step #1: Splitting the ITM into Breakout Models." Breakout models typically include components set to boundary conditions defined via test data, when available, or the uncorrelated ITM. To reduce correlation time, *Veronica* allows these breakout models to be correlated in parallel, and their changes rolled into the full model. Ideally, minimal changes to the full model would be needed after this step. If a component A's error is above tolerance, then the breakout model with A would be re-correlated using boundaries from the updated ITM's predictions.

Using *Veronica*, the VIPER thermal team was able to correlate the ITM on schedule. We team used the 22-week time allotted to us. 14 analysts, with an overall effort of about 8 full time people, contributed to the correlation. The correlation of the TRHE took roughly 15 weeks. Using *Veronica*, we were able to create the "breakout models" and start the correlation process – e.g. starting to correlate the hot case, before the TRHE correlation was finished. After the initial "breakout model" correlation changes were incorporated into the ITM, we achieved an overall Root Mean Square (RMS) error of 7.4C for hot thermal balance and 10C for cold thermal balance. Out of 37 total key components, 56% had RMS errors within 5C and 81% had errors within 10C.

Our paper makes the following contributions: (1) *Veronica*: an approach for integrating mid to large spacecraft thermal models that can significantly speed up the model correlation process by enabling the majority of it to be carried out by multiple analysts in parallel, (2) a description of how Veronica was used to correlate the VIPER ITM, and (3) an overview of model correlation times from a survey of past projects.

BACKGROUND

Correlation Criteria

When a spacecraft ITM is correlated to a thermal balance test, a standard metric used to quantify the quality of the correlation is its overall root-mean-square (RMS) error, defined in Equation 1 [2]. It is typical to have an overall RMS error target of ≤5C [2].

The VIPER thermal team adopted an overall ITM RMS error goal of ≤5C. The VIPER thermal team also specific component error goals, which ranged from <10C to <2C. Each component's error goal was selected based on its importance to the mission, its importance to VIPER's thermal management system, and how close the uncorrelated ITM predicted it was to its Allowable Flight Temperature (AFT) limit during lunar surface operations. For example, the ITM predicted Hazard Cameras operating near their limit so their RMS error target was <2C. Due to schedule constraints, some deviations were accepted in the final correlation.

$$\Delta T_{rms} = \sqrt{\frac{\sum_{i=1}^{n}\left(T_{test(i)} - T_{model(i)}\right)^2}{n}} \quad [1]$$

$T_{test(i)} = T\ at\ position\ i, measured\ by\ a\ TC\ or\ PRT\ on\ a\ component$
$T_{model(i)} = T\ at\ position\ i, interpoltated\ between\ nodes\ using\ a\ TD\ Measure$
$n = number\ of\ positions\ i\ with\ temperature\ sensors\ on\ a\ component$

Observations Behind *Veronica*

This section provides background on the two observations used to develop *Veronica*.

Observation #1: Mid to large spacecraft, typically have different 'thermal zones' that are mostly independent of each other [1]. For example, within VIPER, an insulated 'Warmbox' inside the center rover is independent of the wheel well area and the hazard cameras. However, the hazard cameras exchange a small amount, 0.2W, of heat with the wheel modules.

Observation #2: If component A is not a significant contributor to component B's thermal balance, then the accuracy of A's temperature is not that important when predicting the temperature of B.

We made Observation 2 while conducting sensitivity studies on thermal contacts in the VIPER ITM.[1] We saw about 0.4% of the total heat leaving the MSOLO instrument transfer to its Multi-Layer Insulation (MLI). Then we saw a large 25-35C drop in its MLI only cause a ~3C drop in MSOLO temperatures. To further illustrate Observation 2, consider an example network of 19 nodes shown in Figure 1. Node 1 is heated with a heat load and connected to nodes 2-10 with contacts $G_{1\to2}$ through $G_{1\to10}$. Nodes 2 - 10 each connect to a boundary node.

Seven cases, in Table 1, were solved that illustrate how the changes in nodes 2-10 impact node 1 and vice versa. Figure 1 displays, for Case 1, the breakdown of heat flowing into and out of node 1. In terms of node 1's energy balance, nodes 2-5 are negligible[2], and node 7 is not a significant contributor. Table 1's results demonstrate Observation #2. A large 30C drop in nodes 2-3 has no impact on the network. A large, 29.4C rise in node 7, only has a small impact – increasing node 1 by <0.4C and nodes 9 and 10 by <0.3C. It is less influential than a 4.3C rise in node 8. Also, removing nodes 2-7 only drops node 1 by 0.16C. In a similar manner, nodes that contribute less to node 1's energy balance are less impacted by changes to node 1. A minor 2.63C drop in node 1 has no impact on nodes 2-5, a negligible impact, ≤0.05C, on nodes 6 and 7, a small impact on node 8, and even larger impact to nodes 9 and 10.

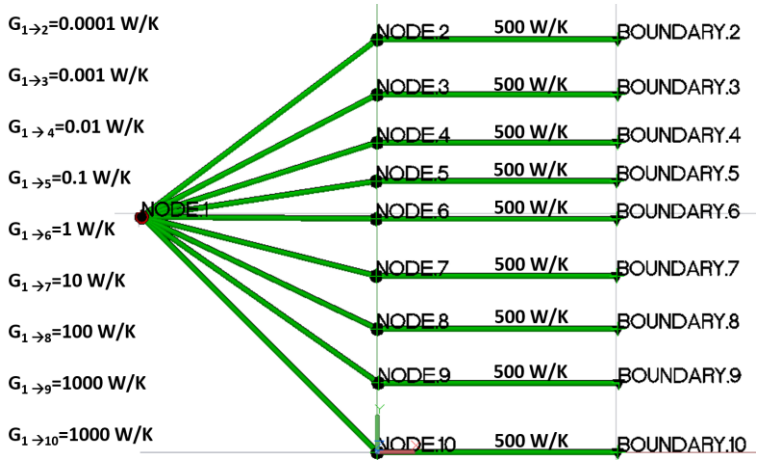

% Heat flowing into – out of node 1
In Case 1, 98.25% of heat in is from the applied load and nodes 8 - 9.

Heat Load	30.80% in
Node 9	53.96% in
Node 8	13.49% in
Node 7	1.59% in
Node 6	0.16% in
Node 10	100% out

Figure 1: Example network for illustrating observation #2.

[1] Note that if a significant heat transfer path from component A is A→B→C, then component C can be a significant contributor to component A's thermal balance even though they are not directly connected.
[2] In fact, removing nodes 2-5 from the network has no impact on the remaining nodes.

Table 1: Example used to illustrate Observation #2.

		Case 1	Case 2	Case 3	Case 4	Case 5	Case 6	Case 7
Node 1 Applied Q [W]		2000	2	2000	2000	2000	2000	2000
Change to Network		-	None	Boundary.2-4 = -20C	Boundary.7 =70C	Boundary.8 = 45C	Boundary .8 = 50C	Removed Nodes 2-7
Node	Case 1 Boundary	T [C]	$\Delta T_{\text{Case 1-Case 2}}$	$\Delta T_{\text{Case 1-Case 3}}$	$\Delta T_{\text{Case 1-Case 4}}$	$\Delta T_{\text{Case 1-Case 5}}$	$\Delta T_{\text{Case 1-Case 6}}$	$\Delta T_{\text{Case 1-Case 7}}$
1	-	29.49	2.63	0	-0.38	-0.54	-1.09	0.16
2	10	10	0	30	0	0	0	-
3	10	10	0	30	0	0	0	-
4	10	10	0	30	0	0	0	-
5	40	40	0	0	0	0	0	-
6	40	39.98	0.01	0	0	0	0	-
7	40	39.79	0.05	0	-29.42	-0.01	-0.03	-
8	40	38.25	0.44	0	-0.06	-4.26	-8.51	0.03
9	40	32.99	1.75	0	-0.26	-0.37	-0.73	0.10
10	10	22.99	1.75	0	-0.26	-0.37	-0.73	0.10

DESIGN

This section describes *Veronica*, a new approach correlating spacecraft thermal models. The main goal of *Veronica* is to enable many analysts in to execute almost all the correlation steps in parallel. This tackles the one of the main reasons that correlation is slow – that its steps are hard to parallelize.

The steps of *Veronica* are: (0) Correlate the test environment (e.g., chamber or makeshift radiation enclosure). This step may not be needed if the environment well known but is important if the test uses custom radiation enclosures heated by slat heaters or IR lamps. (1) Split the spacecraft's ITM into breakout models. (2) Correlate key components in each breakout model using standard correlation practices [1], [2], [12]. Key components refer to components that have a specified RMS error target. (3) Update the ITM to implement the changes needed to correlate each breakout model. (4) Check if the updated ITM meets its error targets. (5) If error targets are not met, repeat steps 2+, for breakout models containing key components whose error targets are not met. In this step, update any boundary conditions that were initially set to temperatures predicted by the uncorrelated ITM. To further speed up the correlation process, portions of these steps can be performed in parallel. For example, step 1 can start before step 0 finishes and step 3 can start before step 2 finishes.

Step #1: Splitting the ITM into Breakout Models

The goal in splitting up an ITM into breakout models is identifying groups of key components that can be grouped together and correlated with negligible impacts to other key components. This is possible if the group's radiative and conductive boundaries conditions can be defined based on test data, since the test data will drive the boundary condition for the correlation. It is also possible if the breakout models are split in different thermal zones that are independent. For example, changes to a conductor impacting the temperature of a rover's wheel will not impact the temperature of a component inside a rover's insulated warm box.

However, not all thermal zones are 100% independent. In this case, we make an optimistic assumption, consistent with Observation 2, that we can split breakout models at contacts with insignificant heat flows. For example, a breakout model for node 1, in the network

that demonstrated Observation 2, could exclude the Boundary 7 node. Node 7 could be set to its uncorrelated temperature predicted by the whole model without negligible impacts to node 1's correlation. Similarly, the node 1 correlation should have negligible impacts on node 7. We identify these contacts with insignificant heat flows by analyzing heat transferred between components in the uncorrelated ITM. In Thermal Desktop this can be done by looking at the output of the built-in SINDA subroutine `submap`.

After key components are grouped into breakout models, the next step is to create each breakout model. The simplest way to create a breakout model is to make a copy of the ITM and use that as the breakout model. However, unless the ITM runs very fast, this approach misses significant savings in correlation time. Therefore, the *Veronica* approach creates each breakout model by making a copy of the ITM, removing un-needed parts until the breakout model runs sufficiently fast (e.g., a few minutes), and setting boundary conditions to define the environment of the breakout model's key components.

The following criteria is used to determine what parts to keep/remove: Include parts that (1) account for the top ~98% of the heat flowing into and ~98% of the heat flowing out of key components[3], or (2) act as reflectors/blockers of radiation between the key components and their radiation environment.

The percent of heat flow into/out of a key component is calculated in Thermal Desktop by parsing the output of the built-in `submap` subroutine. This was done using Equations 2 and 3. where k = a submodel corresponding to a key component, i = a submodel that exchanges heat with k, and $i \rightarrow n$ = submodels included in a breakout model.

$$\text{if TOTAL RATE}_{\text{k,i}} \text{ is positive: } total\ rate\ in_{k,i} = \text{TOTAL RATE}_{\text{k,i}}$$

$$\%In_{k,i} = total\ rate\ in_{k,i} / \sum total\ rate\ in_{k,i} + total\ heat\ rate\ imposed_k$$

$$\%\ of\ Q_{in,k} = \frac{\sum_i^n \%In_{k,i}}{\sum_i^{all} \%In_{k,i}}$$

$$\%\ of\ heat\ flow\ captured_{in} = min\left[\ \%\ of\ Q_{in,k}\ \right] for\ k = 1 \rightarrow\ key\ components\ in\ breakout\ model \quad [2]$$

$$\text{if TOTAL RATE}_{\text{k,i}} \text{ is negative: } total\ rate\ out_{k,i} = \text{TOTAL RATE}_{\text{k,i}}$$

$$\%Out_{k,i} = total\ rate\ out_{k,i} / \sum total\ rate\ out_{k,i}$$

$$\%\ of\ Q_{out,k} = \frac{\sum_i^n \%Out_{k,i}}{\sum_i^{all} \%Out_{k,i}}$$

$$\%\ of\ heat\ flow\ captured_{out} = min\left[\ \%\ of\ Q_{out,k}\ \right] for\ k = 1 \rightarrow\ key\ components\ in\ breakout\ model \quad [3]$$

Other parts are predicted to be 'un-important'. These 'un-important' parts are gradually removed from the model and their impact is replaced with boundary conditions predicted by the uncorrelated ITM. For example, in the network that demonstrated Observation 2, remove the Boundary 7 node and set Boundary 7 to a boundary condition. As parts are removed from the model, its outputs are periodically compared to the ITM. The cutdown process continues until the model runs fast enough but stops if the error between the key components' temperatures gets too high. The allowed error between the breakout model and the ITM should be selected with the desired error for the correlated model. For example, if the desired error for the part is 2C, a ≤0.2C error may be desired.

[3] An alternative approach would be to keep anything contributing to greater than 1% of the total heat transfer. This approach is acceptable if enough of the heat flow into and out of the component is accounted for.

After a breakout model is created, the next step is to adjust its boundary conditions to reflect TVAC data as best as possible. If a boundary surface's temperature is measured, set that bounding surface to that sensor's value. This can be done by changing the nodes directly or adding a boundary node to the model and connecting the bounding surface to the boundary node with a very high conductor. If boundary surface's temperature is not measured but it conducts to a surface whose temperature is measured, then estimate that surface's TVAC temperature with Equation 4:

$$T\_Node = \text{offset from TC} + \text{TC\# from TVAC} \quad [4]$$
$$T\_Node = T\_Node_{ITM\ run} - SENSOR\_TC.\#_{ITM\ run} + \text{TC\# from TVAC}$$

If a boundary surface's temperature is not measured, then set that surface's temperature to the uncorrelated ITM's prediction. Based on Observation 2, the error from doing this will be small if the bounding surface only accounts for a small percentage of heat into or out of the key components. If the bounding surface accounting for a large percent of heat flow than, the error from doing this depends on the error in the ITM.

IMPLEMENTING *VERONICA*

The VIPER thermal team used *Veronica* to correlate the VIPER ITM to hot and cold thermal balance points from a TVAC test conducted at Johnson Space Center's in Chamber A [13]. A full description of the TVAC test is provided by Turk et al. [13]. Hot and cold thermal balance was defined by the following stability criteria: +/-0.2C for components not actively heated by heaters, and a cyclic temperature with a constant period and amplitude for components actively heated by heaters [13].

The VIPER Integrated Thermal Model (ITM)

The VIPER ITM, shown in Figure 2, was developed in Thermal Desktop as a design/verification tool to provide simulations and predictions of the VIPER thermal/fluid performance in identified test and mission environments. The model also provided boundary conditions for the component-level models in support of design/development of VIPER and for the breakout models in support of TVAC correlations.

The ITM was considered a system-level model with the VIPER components simplified based on respective detailed CAD geometry models, or vendor supplied thermal models. The latest ITM version used 20,019 nodes to represent the entire VIPER assembly. The VIPER components were grouped into 97 sub-models that were thermally connected via contactors and conductors.

The ITM included all significant components, instruments, and mechanical assemblies needed for power, communications, navigation, structural support, science, drilling, and mobility. TCS (Thermal Control System) components included Multi-Layer Insulation (MLI), isolators, heaters, thermostats, temperature sensors, radiators, and select optical surface coatings. Additional TCS components included Loop Heat Pipes (LHPs), Constant Conductance Heat Pipes (CCHPs) and thermosiphons.

For the sake of model simplicity, the LHPs were modeled using thermal circuits of one-way conductors. The one-way conductor representation was correlated to component level test data that recreated lunar surface level G-loads on the LHP system of a single heat spreader. FloCAD was not used in this model, because the additional complexity of modeling the 2-phase-flow interactions was not needed. Only the heat transfer provided by, and the temperatures of the LHPs, were what mattered in the ITM.

The ITM was used to assess TCS performance during all mission phases while combined with either the representative lander or Lunar surface model. It also supported the design and execution of several ground tests while combined with the appropriate test facility model. To cut down model size, thermal interactions with the surrounding objects are accounted for using a set of XREFs including the Griffin Lander, Lunar Surface, Launch Vehicle and Thermal Vacuum models. Due to mission requirements, the Lunar Surface model has the capability to assess various surface inclination angles, Rover positions/orientations, plus sun elevation and azimuthal angles.

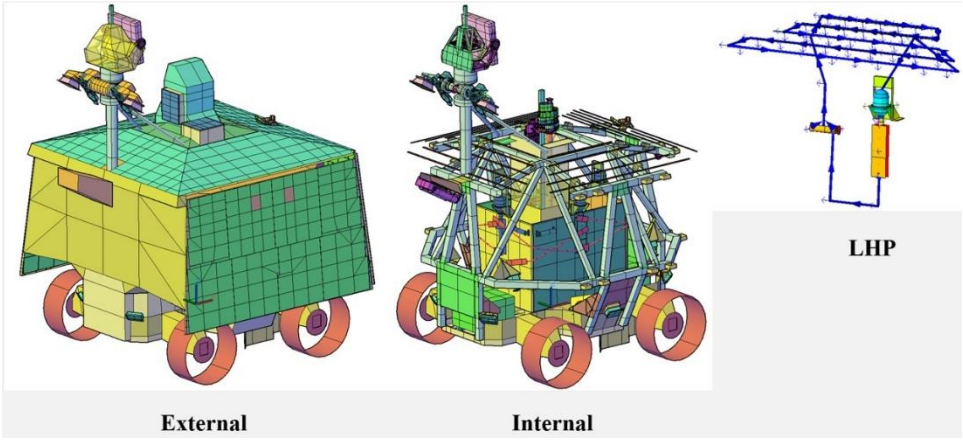

Figure 2: VIPER ITM Thermal Desktop Model.

Veronica **Step 1: Creating Breakout Models**

The VIPER ITM was split into 9 breakout models, listed in Table 2. The LHPs and radiator did not have their own breakout model and were not correlated as part of this effort since they were correlated to a separate test performed in a flight-like gravity orientation.

Table 2 shows that *Veronica*'s approach to simplifying the breakout models produced breakout models that agree well with uncorrelated ITM predictions. Breakout models with ≳98% of heat flows captured, had low RMS errors between their predicted sensor temperatures on key components and uncorrelated ITM prediction. Some breakout models captured <98% of heat flows because we initially used a target of 95-98%. In many cases >98% is captured because breakout models were just simplified until the analyst determined that the model ran fast enough for correlation. The runtime for each model, excluding ray tracing for calculating gray-body exchange factors, is also shown in Table 2. Schedule demanded that some breakout models be built before step 0 was completed for the cold thermal balance case. Therefore, in some cases only values for hot thermal balance values are given. Additionally, the MSOLO and NIRVSS and Warmbox breakout models were re-ran to calculate RMS errors to the uncorrelated ITM.

Table 2. Summary of VIPER breakout models. Unless otherwise noted (1) the RMS error is the highest error out of the cold and hot thermal cases, and (2) the percent of heat flow captured is the lowest out of each key component for both the cold and hot thermal balance cases. ^{H} Designates hot and ^{C}cold thermal balance.

Breakout Model	Key Components	% of Heat flow Captured	RMS error °C to ITM	Approximate SINDA Runtime
Warmbox	Forward Heat Spreader, Aft Heat Spreader, Port Heat Spreader, Starboard Heat Spreader, and their Avionics	>99%	0.5^{H}, 1.2^{C}	~1 minute
Mid-Upper Components	Solar Panels, Aft Cameras, Star Tracker	>99.2%	0.5, 0.06, 0.1	~4 minutes
Hazard Cameras and Lights	4 Hazard Cameras, 6 Hazard Lights	>98%^{H}	0.1^{H}, 0.8^{H}	~6.5 minutes
MSOLO and NIRVSS	MSOLO and NIRVSS science instruments	>99%^{H}	0.85^{H} 1.98^{C}	~10.5 seconds
Gimbal Mast	Gimbal Communication Motors, Navigation Motors, and Navigation Lights	>99%	1.1^{H}, 0.8^{C}	~2.5 minutes
NSS	NSS (enclosed in the Front Panel MLI)	100%, >99% Front Panel MLI ^{H}	0.4^{H}	~6.5 minutes
Batteries	Aft Battery, Forward Battery	>95%	0.8^{H} 4.8^{C}	~30 seconds
Wheel Well	Wheel Module, Mobility Module	>98%	0.12	~4.5 minutes
External Bottom	Rover kits, Rover release mechanisms	>97% of heat in, >99% of heat out	1.8^{H} 2.0^{C}	~2.2 minutes

For brevity, we only walk through the creation of 1 breakout model in detail and provide a brief description of 3 others.

Wheel Well Breakout Model: To create this model, the first step was to run the uncorrelated ITM with ‘call submap()’ added to the Logic Manager in the Operations Block Post Solution (TDPOSTSL) logic block. This instructs SINDA to tally the heat flows between all submodules and place it at the end of the .out file. The .out file and .cc file were used as inputs to a Python script. For each submodel, the Python script sorted the heat flows listed in the submap output from largest to smallest, found conductors/contactors that connected those submodels, and outputted the results to an Excel file. Figure 3 displays this output for the submodel WHEEL_MODULE for hot thermal balance. This step was repeated for cold thermal balance.

The second step was to list the submodels that are important to capturing 95% and 98% of the heat flowing into/out of the Wheel Well submodels. This list is shown in Table 3. The list also includes submodels important to the MLI Lower Structure and the Structure Lower Chassis, since they were both important to submodels in the Wheel Well. Additionally, the Structure Lower Chassis was not well instrumented, so it was desired to have the breakout model calculate its temperature as opposed to bounding it to temperatures predicted by the uncorrelated ITM.

Next, components not in Table 3 that were not needed to block/reflect radiation from the thermal vacuum enclosure to the Wheel Well were removed. For calculating the error between the breakout model and the ITM, all parts except the Wheel Well submodels, the MLI Lower Structure, and Structure lower chassis were bound to uncorrelated ITM temperatures. At this point the breakout model did not run fast enough. The final version also removed the following

parts from Table 3: Haz Lights, Trident_LL, Trident_Structure, MLI_Warmbox, and upper pieces of the Structure Frame. Removing unneeded frame cut model runtime by 3.3 minutes. The completed Wheel Well breakout model is shown in Figure 4.

Hot Thermal Balance												
	A SUBMAP OF THERMAL SUBMODEL WHEEL_MODULE											
AVERAGE DIFF/ARIT TEMP.	=	51.529	(DEG)									
AVG. BDY/HTR NODE TEMP.	=	(NONE)	(DEG)									
TOTAL CAPACITANCE	=	17869	(ENERGY/DEG)									
TOTAL HEAT RATE IMPOSED	=	0	(ENERGY/TIME)							Sum	96.45	97.86
TOTAL HEAT TO INTL BDYS.	=	0	(ENERGY/TIME)							SUM	98.2	99.48
SUBMODEL	TYPE	AVG TEMP.	LIN/TIE COND	HEAT RATE TO	RAD. COND.	HEAT RATE TO	TOTAL COND.	TOTAL RATE	total rate out	total rate in	% Out	% In
SPACE	THERMAL	(NONE)	0	0	0.1423	88.827	0.35444	88.827	88.827	0	94.12	0
TV_RAD_ENCL_STBD	THERMAL	111.06	0	0	0.0441616	-37.51	0.4862	-37.51	0	37.51	0	39.75
TV_RAD_ENCL_BTTM	THERMAL	65.97	0	0	0.31964	-27.824	2.7761	-27.824	0	27.824	0	29.48
TV_RAD_ENCL_PORT	THERMAL	72.9	0	0	0.097658	-14.768	0.91143	-14.768	0	14.768	0	15.65
TV_RAD_ENCL_AFT	THERMAL	69.23	0	0	0.0781323	-6.2872	0.71682	-6.2872	0	6.2872	0	6.66
TV_RAD_ENCL_FRONT_BTTM	THERMAL	58.26	0	0	0.0254243	-5.9599	0.21842	-5.9599	0	5.9599	0	6.32
STRUCTURE_LOWER_CHASSIS	THERMAL	52.58	12.967	2.2323	0.058946	-0.0297921	13.448	2.2025	2.2025	0	2.33	0
WHEEL_MODULE_STEERING_MOTORS	THERMAL	54.52	98.248	-0.91587	0.000380693	-0.00363376	98.251	-0.91951	0	0.91951	0	0.97
SOLAR_PANEL_STRBD	THERMAL	-11.79	0	0	0.00476169	0.86518	0.0331745	0.86518	0.86518	0	0.92	0
MLI_LOWERSTRUCTURE	THERMAL	53.67	0	0	0.37664	-0.61341	3.1435	-0.61341	0	0.61341	0	0.65
TV_OVERHEAD_STRUCTURE_CROSS_BARS	THERMAL	-126.76	0	0	0.00059307	0.35209	0.00205152	0.35209	0.35209	0	0.37	0
HAZ_CAMERA	THERMAL	40.8	0	0	0.00193343	0.22056	0.0149249	0.22056	0.22056	0	0.23	0
MLI_FRONT_PANEL	THERMAL	-14.53	0	0	0.000544641	0.21565	0.00289431	0.21565	0.21565	0	0.23	0

Figure 3: Output of Python script the gives lists heat flows and linear contacts that connect to the Wheel Module. Note: “Heat Rate To” is positive if heat flows from the WHEEL_MODULE to the submodel in the list.

Table 3 Submodels that catpure for 98% of heat into or out of Wheel Module, Wheel Module Drive Motors, Wheel Module Steering Motors, Wheel Module Susp Motors, MLI Wheel Module, Structure Lower Chassis, MLI Lower Structure. Only pairs in blue are needed for 95%. Submodels in the Wheel Well are not listed.

Important submodels:	Important to:
BATTERY	STRUCTURE_LOWER_CHASSIS, WHEEL_MODULE_SUSP_MOTORS, MLI_LOWER STRUCTURE
HAZ_CAMERA	WHEEL_MODULE, MLI_WHEELMODULES, MLI_LOWERSTRUCTURE
HAZ_LIGHTS	MLI_LOWERSTRUCTURE
HS_STANDOFFS	WHEEL_MODULE_SUSP_MOTORS, STRUCTURE_LOWER_CHASSIS
MLI_FRONT_PANEL	WHEEL_MODULE, MLI_LOWERSTRUCTURE
MLI_LOWERSTRUCTURE	WHEEL_MODULE, MLI_WHEELMODULES, STRUCTURE_LOWER_CHASSIS
MLI_OCTAGON	WHEEL_MODULE_SUSP_MOTORS. STRUCTURE_LOWER_CHASSIS, MLI_LOWERSTRUCTURE
MLI_WARMBOX	WHEEL_MODULE_SUSP_MOTORS, STRUCTURE_LOWER_CHASSIS, MLI_LOWERSTRUCTURE
MLI_WHEELMODULES	WHEEL_MODULE, WHEEL_MODULE_DRIVE_MOTORS, WHEEL_MODULE_STEERING_MOTORS, STRUCTURE_LOWER_CHSSIS, MLI_LOWER_STRUCTURE
MSOLO, ROVER_KITS	WHEEL_MODULE_SUSP_MOTORS, STRUCTURE_LOWER_CHASSIS
SOLAR_PANEL_AFT, SOLAR_PANEL_PORT	WHEEL_MODULE, MLI_LOWERSTRUCTURE
SOLAR_PANEL_STRBD	WHEEL_MODULE, MLI_WHEELMODULES, MLI_LOWERSTRUCTURE
STRUCTURE_FRAME	STRUCTURE_LOWER_CHASSIS , MLI_LOWERSTRUCTURE
STRUCTURE_LOWER_CHASSIS	WHEEL_MODULE_SUSP_MOTORS, MLI_WHEELMODULE, MLI_LOWERSTRUCTURE
MLI_DRILL, MLI_MSOLO	STRUCTURE_LOWER_CHSSIS
NIRVSS, PWB_FWD, PWB_AFT, RRM_FLAPS, TRIDENT_STRUCTURE, TRIDENT_LLL	STRUCTURE_LOWER_CHASSIS
TV_CART	MLI_WHEELMODULES, MLI_LOWERSTRUCTURE, STRUCTURE_LOWER_CHASSIS
TV_OVERHEAD_STRUCTURE_CROSS_BARS	WHEEL_MODULE
TV_RAD_ENCL_AFT, TV_RAD_ENCL_BTTM, TV_RAD_ENCL_FRONT_BTTM, TV_RAD_ENCL_PORT, TV_RAD_ENCL_STBD, TV_RRM_SCARFF, TV_RRM_STRUCTURE	WHEEL_MODULE, MLI_WHEELMODULE, MLI_LOWERSTRUCTURE, STRUCTURE_LOWER_CHASSIS
TV_RAD_ENCL_FRONT_TOP	MLI_LOWERSTRUCTURE

After checking that the breakout model's predictions agreed with the uncorrelated ITM, the last step was to change the boundary conditions to reflect measured TVAC temperatures. Since there were not many TCs on the frame, Equation 4 was used to bound the bottom horizontal frame pieces to estimated test temperatures.

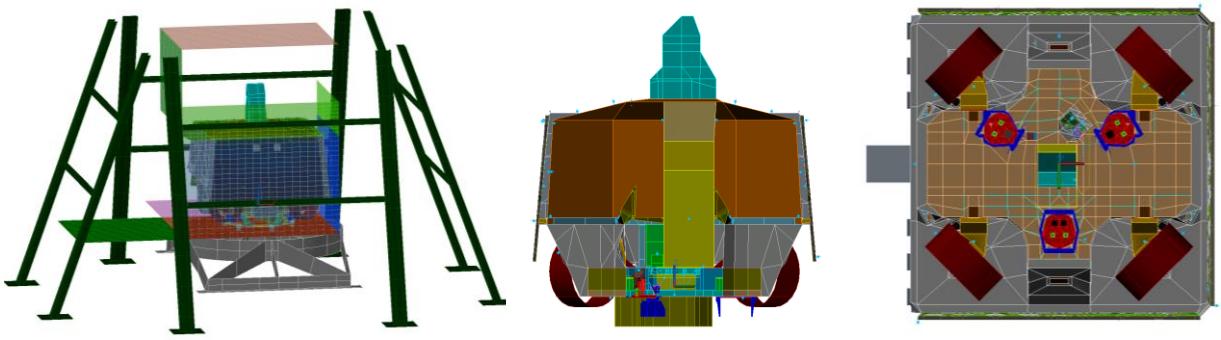

Figure 4: Wheel Well Breakout Model, cut-away aft view (center), bottom view (right).

Hazard Camera and Light Breakout Models: Figure 5 depicts the Hazard Cameras and Hazard Lights breakout model. The model excludes the radiators, LHPs, science instruments, drill components, and everything inside the Warmbox. Its boundary conditions were provided by: (1) the MLI enclosures, (2) the lower chassis, (3) the entire thermal vacuum radiation enclosure, (3) the battery, and (4) upper and lower horizontal structure frame pieces that support the solar panels. Due to lack of TCs on the lower chassis, the lower chassis was bounded to its temperatures predicted by the uncorrelated ITM. The upper frame was a major contributor to the Hazard Cameras' temperatures. Like in the Wheel Well Breakout Model, Equation 4 was used to bound the horizontal frame pieces to estimated test temperatures.

MSOLO and NIRVSS Breakout Model: Figure 6 depicts the breakout model for two science instruments: MSOLO and NIRVSS. The model contains the MSOLO and NIRVSS, their MLI, their support brackets, and their thermosiphon flanges. It also contains elements of the structure lower chassis that conduct to the MSOLO and NIRVSS and the bottom of the thermal vacuum enclosure. Its boundary conditions are provided by: (1) the thermosiphon flanges, (2) MLI surrounding the MSOLO and NIRVSS, (3) a sink temperature, calculated with the uncorrelated ITM, for the exposed section of the MSOLO snoot, (4) part of the structure lower chassis, and (5) the bottom panel of the TRHE.

Warmbox Breakout Model: Figure 7 depicts the Warmbox breakout model. This model contains the rover's internal avionics mounted to heat spreaders in the Warmbox. It also contains CCHPs which connect the heat spreaders. The model's boundary conditions are provided by the Warmbox MLI, drill MLI, LHP evaporator flanges, and heat loads that applied the heat transferred from the battery to the heat spreaders via thermal straps.

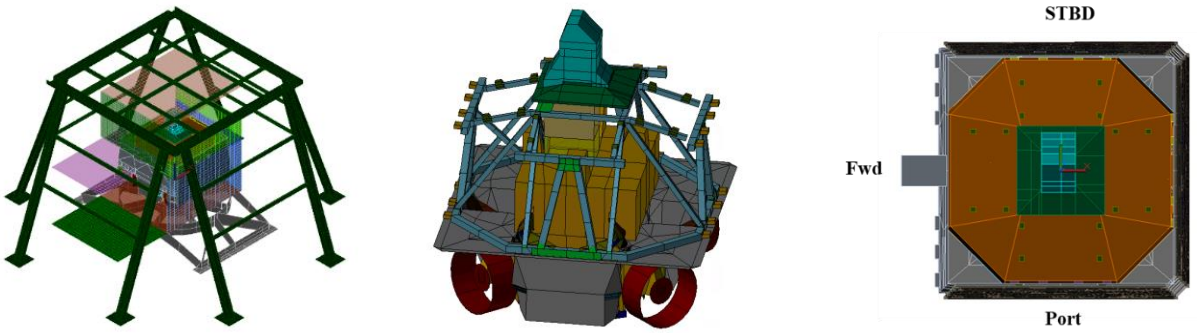

Figure 5: Hazard Cameras and Hazard Lights Breakout Model, inside view (center), top view (right).

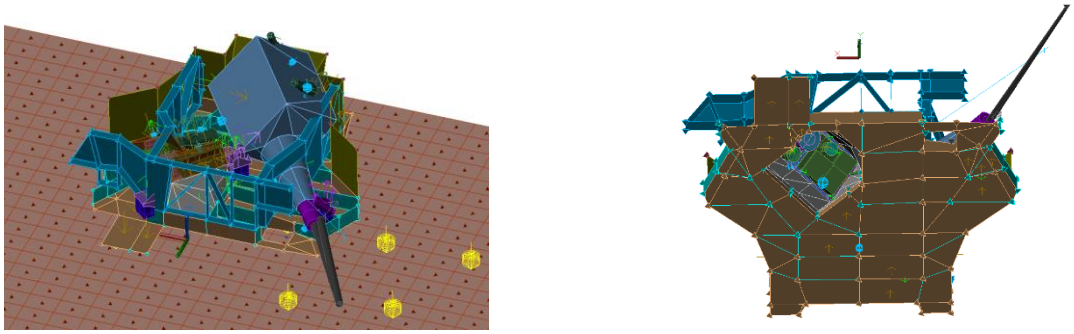

Figure 6: MSOLO and NIRVSS Breakout Model.

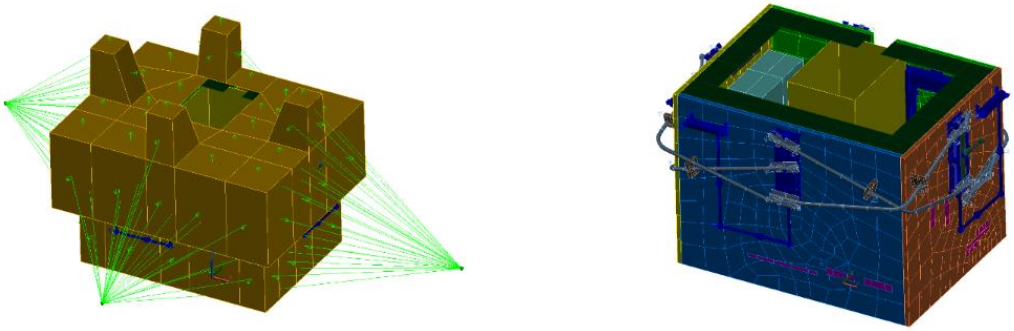

Figure 7: Warmbox Breakout Model. MLI (left image) surrounds heat spreaders (right image) which are connected by CCHPs (in light blue) and cooled by LHPs (dark blue).

Veronica **Step 2: Correlating the Breakout Models**

The breakout models were correlated in parallel by a group of analysts using standard correlation practices. The main model parameters investigated during correlation were (1) component heat dissipations, (2) conductances between parts, (3) MLI effective emittances, and (4) model geometry (i.e., did geometric simplifications or incorrect TD measure placement contribute to deviations from test predictions?). During correlation, parameters were only allowed to change within realistic bounds based on their expected uncertainties.

Correlation was performed with steady state runs. Each analyst was provided a common list of hot and cold steady state temperatures to correlate to. The steady state temperatures were 10 minute averages taken at the end of each thermal balance segment.

To correlate using steady state runs, component and heater dissipations were updated based on TVAC data. Component dissipations were modeled with heat loads. Their values came from direct and derived telemetry sources measured during the test. Any gaps were filled in with the values from the power equipment list, which was informed by box level tests on engineering development units or flight spares of hardware. Heaters were modeled using Thermal Desktop's heater 'Power Percentage' option, which supplies a constant heater power based on the percent of time the heater would be on during transient operation. In other words, for each heater, the model supplied a constant heat load which equaled the heater's duty cycle seen during the thermal balance portion of the test × its total power. Since standard correlation practices were used to correlate each breakout model we only describe the Warmbox breakout model correlation in detail.

Correlating the Warmbox Breakout Model: To speed up correlation, the Warmbox breakout model was correlated using a two-step approach similar to the *Veronica* method but without the creation of breakout models for the individual heat spreaders. (Step#1) Instead, 4 copies were made of the Warmbox breakout model. Each copy was assigned to a different analyst who correlated an individual heat spreader. (Step#2) Next, a single analyst updated the Warmbox breakout model and correlated it to TVAC data. Step#2 was needed because the heat spreaders are designed in a way so that they are tied together to further alleviate heat dissipation needs rather than solely relying on themselves individually. This meant that changes made to any heat spreader for correlation affected the neighboring heat spreaders as well.

(Step #1) The following changes were made to correlate the heat spreaders. Many changes were made to better match the heat spreaders' test temperature gradients. Each change made to a heat spreader was only made in the model used to correlate that heat spreader.

- Updated component heat dissipations and boundary temperatures based on further post-processing of TVAC.
- Checked sensor locations and values for correctness. Multiple sensor locations were fixed and several bad or incorrectly reported sensor temperatures were identified.
- Added a necessary sensor for the Trident Avionics box to the forward heat spreader. This required an independent component level correlation to derive internal conductances.
- Added a boundary condition in the form of a heat load to capture heat exchange from the Fwd Battery's thermal straps. The heat load equaled the strap's conductance times the temperature delta across the strap measured during thermal balance.
- Refined the Fwd LHP mounting plate's mesh resolution.
- Updated Fwd and Aft embedded heat pipes by adding additional logic to better match the behavior seen over the entire length of pipe seen in VIPER TVAC.
- Adjusted Aft heat spreader's condensing and evaporating constants for a crossing CCHP.
- Increased fidelity of the transceiver's sensors to account for the fact that its interior conductance was unknown.
- Separated Aft and Port LHP contactors to change their coefficients to improve heat exchanges.
- Reduced the number of boundary nodes in the Port LHP's evaporator and mount plates. The initial high number of boundary nodes was overdriving the solution leading to additional error.
- Adjusted Stbd heat spreader condensing and evaporating constants for certain embedded heat pipes.

(Step#2) During this step, the Warmbox breakout model was slowly modified to implement changes made to the 4 models during Step#1. These changes were implemented one heat spreader at a time for two reasons. 1) The first was to verify changes were implemented correctly. This was done by calculating the RMS errors of the Warmbox before and after implementing changes for each heat spreader and comparing these to the RMS errors of the individual correlated heat spreader models. 2) The second was to observe the degree to which each heat spreader correlation changed the overall Warmbox error. Observing this helped lead the analyst to parts of the model to target to improve the overall Warmbox's correlation.

Additionally, the slow integration approach enabled additional errors and/or mistakes that may have gone unnoticed to be found and solved. For example, an incident on the Port heat spreader was noticed during individual heat spreader correlations where a crossing CCHP sensor was considerably off from its target which caused large errors. The CCHP connected the Port and Aft heat spreaders, but no efforts on the Port correlations caused the error to decrease which lead to a note for the re-integration analyst to monitor when Aft correlations were implemented. During re-integration, the error was not successfully mitigated by the Aft changes leading to a deeper investigation. However, a solution was found with the sensor being noted as a bad sensor during VIPER TVAC testing due to the data recordings witnessed and was thus thrown out of correlation efforts which eliminated the error.

Figure 8 displays RMS errors from Steps #1 and #2. A good Warmbox breakout model correlation was achieved with RMS errors ≤2.1C, except for the IMU. However, the TC on the IMU showed an unrealistically large, >20C, offset between the TC and an internal sensor, which were <10C apart during component level TVAC tests. Therefore, the IMU TC reading was determined to be incorrect. With other nearby components and sensors to the IMU successfully correlated, and with the understanding that the IMU heat dissipation does not greatly affect other nearby components, the IMU was considered successfully correlated by proxy.

Overall, the *Veronica*-like approach used to corelate the Warmbox proved to be efficient and an effective use of the analysts' time to produce desirable results in an unusual manner. During regular meetings, the analysts tasked with the heat spreader correlations were able to discuss and split the load in testing broad changes that could majorly affect errors seen which allowed for even faster correlations as opposed to a singular analyst taking the same approach. The overall correlation took roughly 200 hours with about 80 hours used for Step#2.

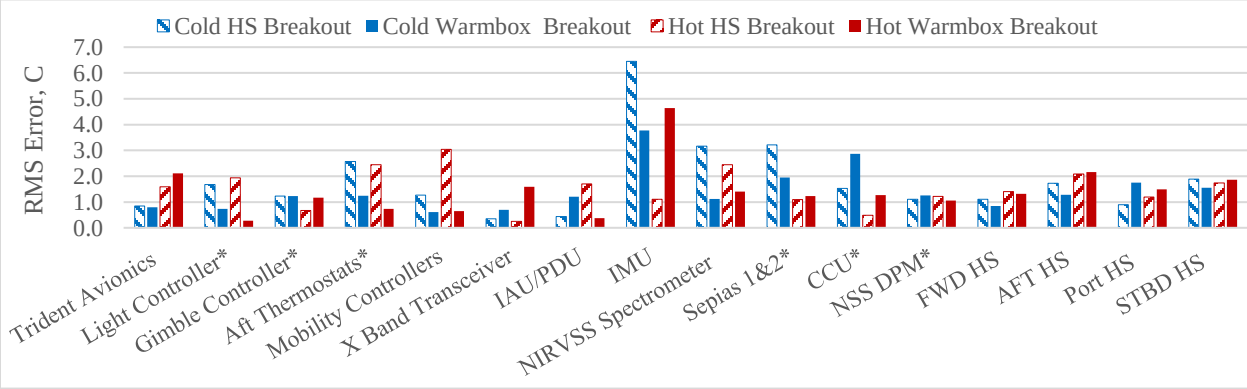

Figure 8: Error comparison between the individual heat spreader correlations, denoted as HS breakout, and the overall Warmbox correlation. *Denotes an un-instrumented component where the nearest sensors are compared.

***Veronica* Step 3 - 5: Correlating the ITM**

After each breakout model was correlated, its changes were rolled into the ITM and the ITM's RMS error was calculated. This was the version of the 'correlated' ITM at the used for requirements verification prior to the project ramping down.

Figure 9 shows how well correlated ITM and correlated breakout models compared in terms of RMS error. In the correlated breakout models, 28 and 33 components met their RMS error goals at cold and hot thermal balance, respectively. In the ITM, these numbers dropped to 20 and 22 components for the cold and hot thermal balance tests. However, as shown in Table 5, Figure 10, and Figure 11, there was a significant reduction in model error between the uncorrelated and correlated ITM. For hot and cold thermal balance, 1.6 and 2.2 times more components reached their error goals, and the RMS error dropped 4.8C and 4.7C, respectively.

The increase in error from the breakout models to the ITM may be due to the construction of the breakout models, in addition to any error from correlating the breakout models in parallel. For example, the battery breakout had a nearly 5C lower RMS error than the ITM in the cold case, and Table 4 shows that the battery breakout model had a 4.8C RMS error between itself and the uncorrelated ITM. Additionally, several of the breakout models were created before the TRHE correlation was finished. Updates to the ITM and the TRHE were still being rolled in while the breakout models were being constructed. For example, several gaps and a slight panel angle were added to the TRHE to better reflect the test after the breakout models were correlated. This change generally caused some components in the ITM to increase in error and some to decrease. Also, further updates to the logic governing LHP operation led to significant changes in radiator temperature, which had an impact on the mast/gimbal temperatures in the correlated ITM. This ultimately led to inconsistencies between the correlated ITM and breakout model mast/gimbal components.

Following re-integration of the breakout models into the ITM, the team entered a "Sustainment Team" phase. This phase is ongoing and includes several efforts to improve fidelity of the ITM and reduce RMS errors with comparison to testing results.

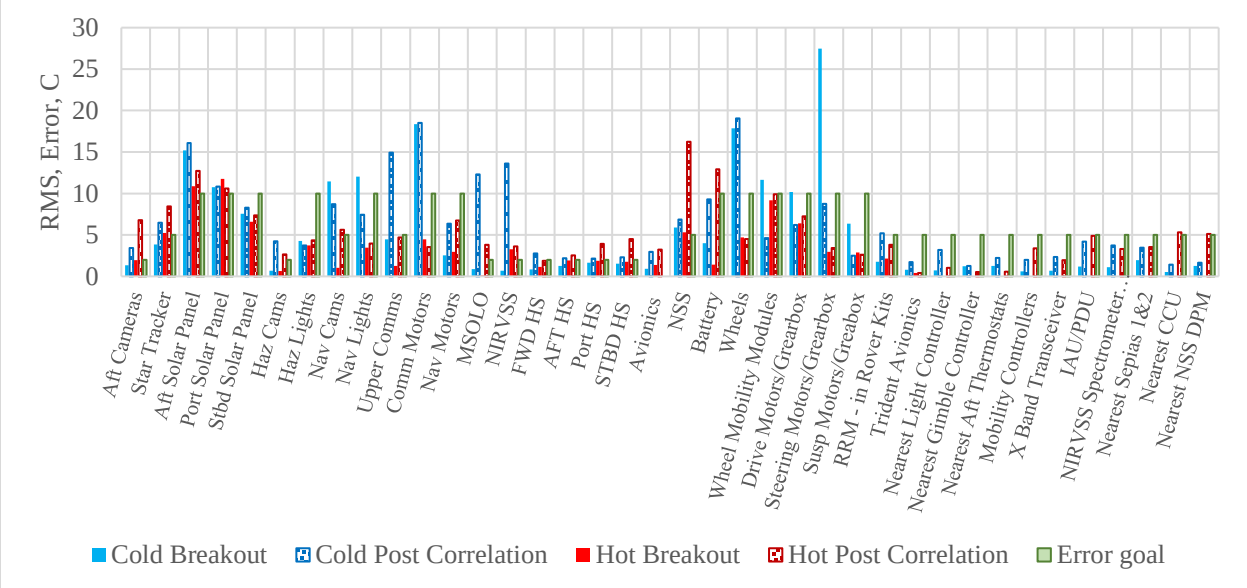

Figure 9: Error comparison between key component groups. Breakout denotes error from the breakout models. ITM denotes the ITM after the breakout model correlations were incorporated into the ITM, with no other changes.

Table 5: ITM correlation metrics before correlation and after incorporating changes from breakout models.

Pre-Correlation	*14.78 C*		***Total RMS Cold***	*12.12 C*		***Total RMS Hot***
	# Sensors Colder		***# Sensors Hotter***	***# Sensors Colder***		***# Sensors Hotter***
	124		*71*	*80*		*115*
	% <5C RMS	***% <10C RMS***	***% Within Goal***	***% <5C RMS***	***% <10C RMS***	***% Within Goal***
	35%	65%	32%	22%	46%	27%
Post-TRHE Correlation	*17.66 C*		***Total RMS Cold***	*11.75 C*		***Total RMS Hot***
	# Sensors Colder		***# Sensors Hotter***	***# Sensors Colder***		***# Sensors Hotter***
	120		***75***	*101*		***94***
	% <5C RMS	***% <10C RMS***	***% Within Goal***	***% <5C RMS***	***% <10C RMS***	***% Within Goal***
	43%	62%	35%	16%	51%	19%
Post-Correlation	*9.99 C*		***Total RMS Cold***	*7.44 C*		***Total RMS Hot***
	# Sensors Colder		***# Sensors Hotter***	***# Sensors Colder***		***# Sensors Hotter***
	88		*107*	*88*		*107*
	% <5C RMS	***% <10C RMS***	***% Within Goal***	***% <5C RMS***	***% <10C RMS***	***% Within Goal***
	54%	81%	54%	65%	89%	59%

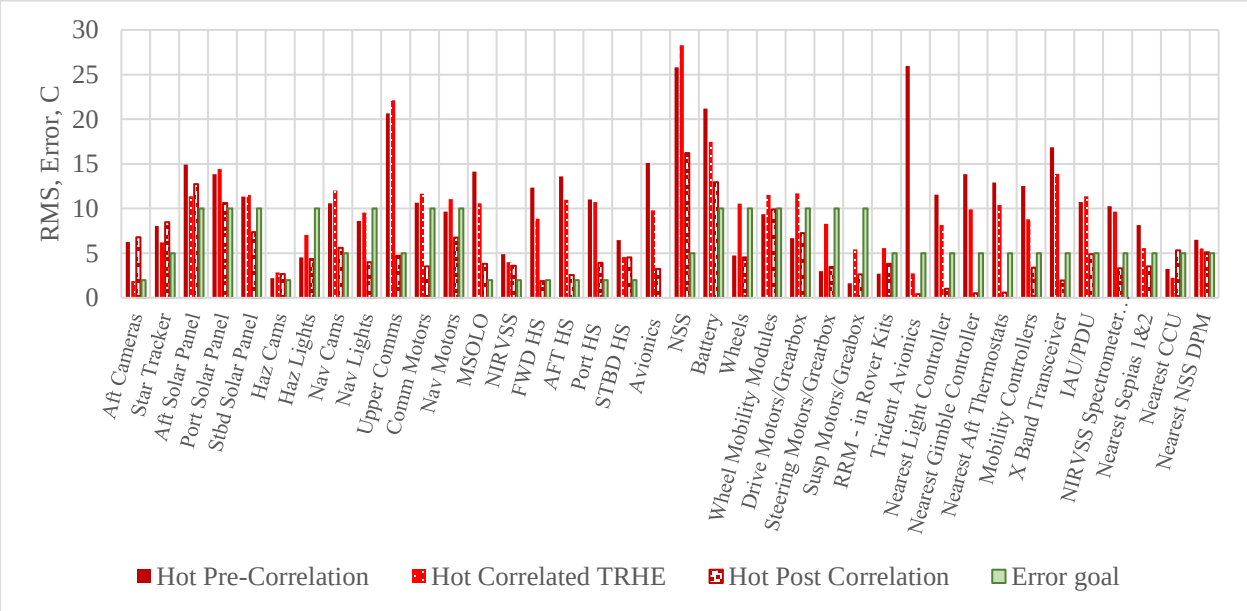

Figure 10: Reduction in hot thermal balance model error from correlation effort.

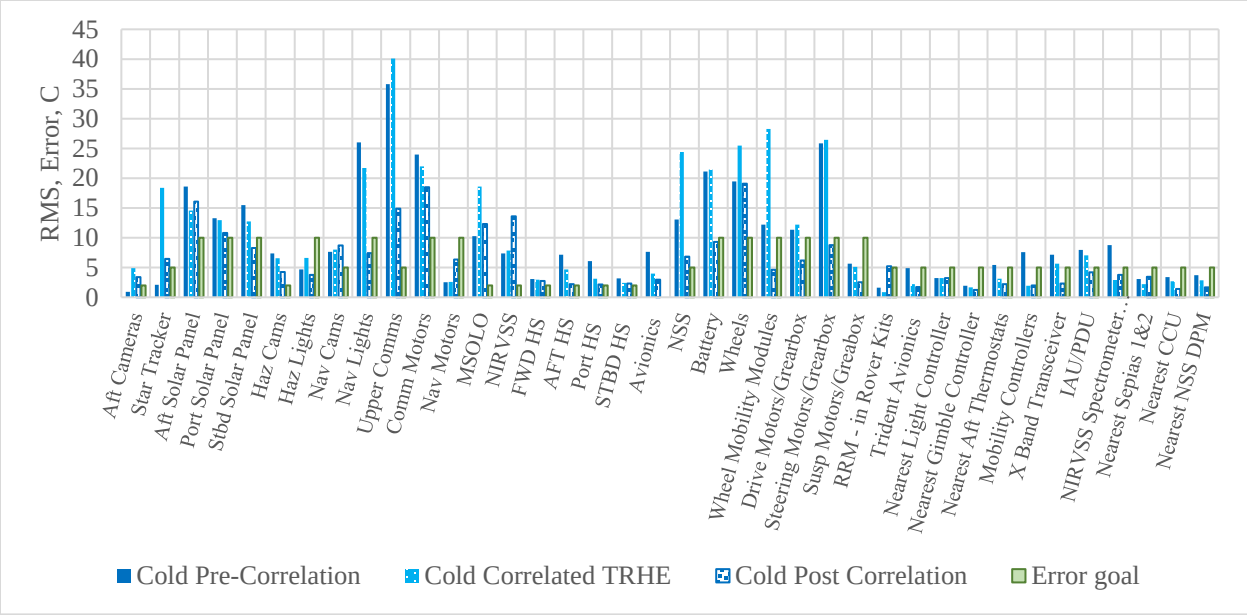

Figure 11: Reduction in cold thermal balance model error from correlation effort.

MODEL CORRELATION TIME SURVEY

While model correlation has a reputation for being slow. There is very little public information about thermal model correlation times for real systems. Since we believed this information would be useful for future projects, we reached out to the thermal community to inquire about model parameters and correlation times for past projects.

Table 6 presents the data we gathered. Figure 12 through Figure 15 plot model correlation times verses different model complexity parameters. There is a lot of scatter in the plots. We do not see a predictable relationship between the model characteristics in Table 4 and correlation times. However, there is a general trend that correlating smaller, simpler models (e.g. tile models and breakout models) take less time than larger, more complex models (e.g. Orion).

Scatter in correlation times is influenced by several factors. Some models were more mature or had a higher fidelity than others when going into test. The VIPER ITM was still undergoing updates leading up to and after TVAC. Updates included changes to the ITM itself, to improve fidelity, and the TRHE, since the TRHE was correlated post TVAC. The complete uncorrelated version of the ITM was available 11 weeks post-test. Alternatively, other projects, e.g., Orion, were able to shorten post-test correlation time by starting during TVAC. Additionally, some models, such as SAGE III, were correlated to more test segments. SAGE III was correlated to an unpowered and powered hot and cold thermal balances, hot and cold cooldown from a powered to an unpowered state, plus several functional tests [14]. Moreover, the number of analysts working model correlation and the fraction of their time spent on model correlation varied. Several models had less than one person's effort dedicated to them.

Table 6: Model parameters and correlation times for past projects. [manual] = a manual correlation effort[4]. Models were in Thermal Desktop unless otherwise marked. Assumes 1 month = 4.3 weeks. <1 indicates one less than full time individual. # Points = number of test segments correlated. Blanks cells occur when data was not available.

Model	Approx. Correlation Time (weeks)	# Nodes	TD submodels	# Contacts	# heaters & heat loads used	# Correlated Sensors	Approx. full-time people	# Points
JWST Aft Optics Subsystem (AOS) [manual]	0.4					39.0	3	1
Tile Radiation Test 1	1.3	3500	11	122	1	11.0	1	3
JWST ISIM Electronics Compartment (IEC) [manual]	2.0	7590				180.0	5	1
Tile Radiation Test 2	4.0	3700	11	122	1	11.0	1	3
MMPACT terrestrial arm [14]	6.0	9830		59	73	44.0	1	1
Tile Conduction Test	6.3	6113	14	95		5.0	1	3
Surface Water and Ocean Topography (SWOT) Satellite (in Simcenter) [manual] [5]	8.6			32		118.0	1	3
JWST Core [manual]	12.9	24000				512.0	15	2
NISAR instruments and Reflector	12.9	100000	350	900	250	250.0	2	2
Orion Crew Module and ESA Service Module[5]	12.9	184764	407	13565	639	872.0	~9	3
Flow Boiling and Condensation Experiment	12.9	13399	14	240	4	17.0	<1	2
High Efficiency Megawatt Motor – Superconducting Rotor (in COMSOL)	12.9		N/A			21.0	<1	1
Europa Clipper (2024 correlation)	12.9	47909	261	4927	111.00			
Mars 2020 Rover (2019-2020 correlation)	12.9	12023	133	1616	150.00			
Mars 2020 Stacked Vehicle (Cruise, Descent, Aeroshell, and Simulated Stowed Rover, 2019 correlation). [15]	17.2	20323	211	1330	34.00			
SAGE III ISS Payload [16]	21.5	9340	9	427	21	100.0	<1	7+
VIPER (overall rover)	22 (13[6])	20019	97	1327	186	141.0	8	2
VIPER Thermal Radiation Enclosure (TRHE)	15.05	7868	38	60	149	160.0	1	2
VIPER: Mid-Upper Breakout (including solar panels, aft cams, and star tracker)	4	8890	36	166	40	27.0	1	2
VIPER: Mast-Gimbal Breakout	2.19	1291	19	102	18	22.0	1	2
VIPER: Haz Cam/Haz Light Breakout	1.25	2371	43	61	8	10.0	1	2
VIPER: Wheel Well Breakout	1.4	1352	54	131	21	45.0	1	2
VIPER Battery Breakout	0.45	314	10	28	4	14.0	1	2
VIPER Warmbox Breakout	2.25	3743	34	126	56	59.0	4	2
Viper Fwd Heat Spreader Breakout	3	718	5	20	10	16.0	1	2
VIPER MSOLO/NIRVSS Breakout	8	430	9	37	10	8.0	<1	2
VIPER NSS Breakout	3	247	32	13	5	9.0	1	2

[4] The JWST team also developed and implemented a custom semi-automated correlation process [11]. This dropped the model correlation times of the AOS, IEC, and Core, to ~1 hour, 4 days, and 2 weeks with people running autogenerated cases in parallel.

[5] The Orion correlation effort started during TVAC and TVAC time is excluded.

[6] Time between VIPER ITM with correlated THRE delivery and March 2025 correlation completion.

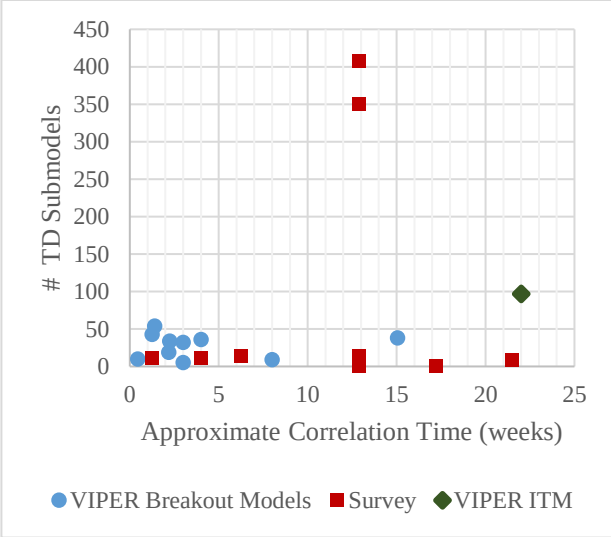

Figure 12: Approximate correlation time verses model complexity in terms of number of Thermal Desktop (TD) submodels. VIPER ITM time includes 9 weeks of overlapping time to correlate the TRHE.

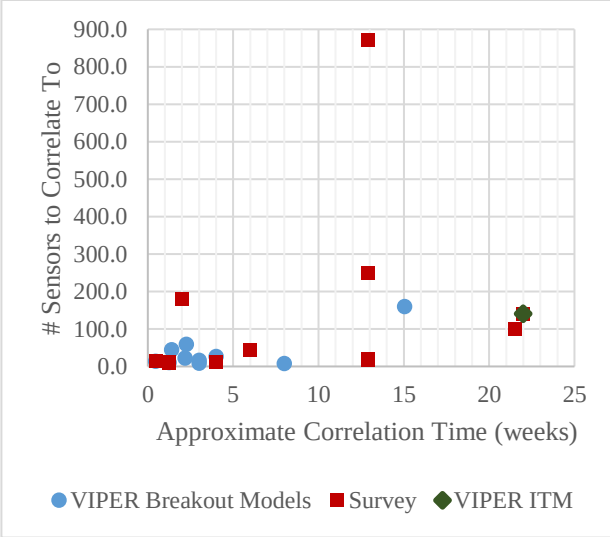

Figure 13: Approximate correlation time verses model complexity in terms of sensor count. VIPER ITM time includes 9 weeks of overlapping time to correlate the TRHE.

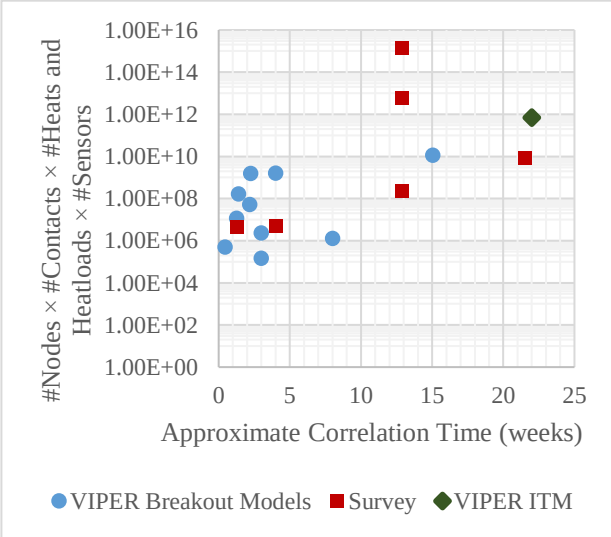

Figure 14: Approximate correlation time verses model complexity in terms of a multiplication of model parameters. VIPER ITM time includes 9 weeks of overlapping time to correlate the TRHE.

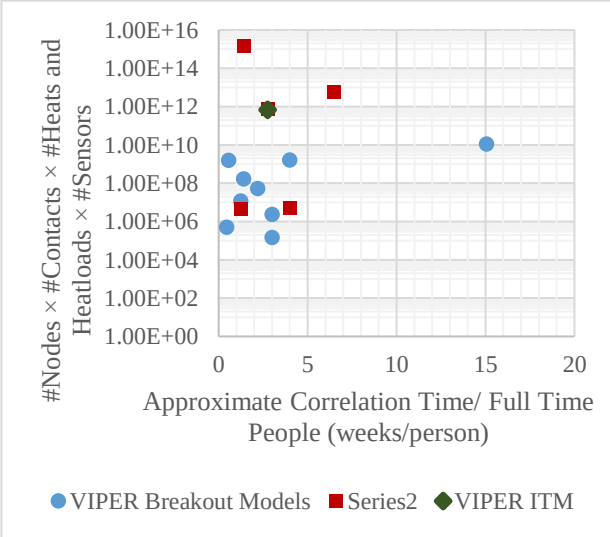

Figure 15: Approximate correlation time pers person verses model complexity in terms of a multiplication of model parameters. VIPER ITM time includes 9 weeks of overlapping time to correlate the TRHE.

RELATED WORK

Optimization Algorithms: Many works have aimed to speed up model correlation by using optimization algorithms to find a set of model parameters (i.e., contact conductances, MLI ε*s) that minimize model error with in as few iterations as possible [6], [7] , [8] , [9], [10]. Optimization algorithms have been used for correlating instruments [6], [7], satellites [17], [5] [18], and large subsystems within the James Webb Space Telescope (JWST) [11]. However, these algorithms cannot address model errors due to missing contacts, incorrect geometry (i.e.

due to oversimplification) [6], [19], [11]. *Veronica* does not attempt to replace these methods but instead presents another option for speeding up correlation – by enabling a large model to be split up and mostly correlated in parallel.

Veronica's use of small breakout models can make using these algorithms faster and easier. Optimization algorithms converge on solutions faster with smaller models with less model parameters and temperature sensors [8]. Algorithms that are good at accidently finding local optimums[7] have not been proven in large thermal models with thousands of model parameters [11]. Others, like those used when correlating JWST, can accidently find local minimum and require a manual sensitively analysis to confirm results [11]. Such sensitivity studies could be conducted faster using breakout models.

Leveraging Reduced Order Models: Hengeveld and Multon proposed using reduced order models (ROMs) to speed up model correlation [4]. Since ROMs run faster, correlated model parameters can be identified quicker [4]. Cato et al. implemented a similar concept when correlating the JWST Core subsystem – by creating faster running model to use for correlation [11]. *Veronica* also leverages the fact that smaller models can be correlated faster – except instead of using ROMS, it uses breakout models, which are pieces of the whole model.

CONCLUSION

This paper presented the *Veronica*, a new approach that uses the uncorrelated ITM's heat flow predictions to breakout the ITM into "breakout models" which are correlated in parallel prior to the final ITM correlation. By correlating mostly independent breakout models first, the time and effort needed to finish correlating the full ITM can be reduced.

Veronica was developed by the VIPER thermal team to correlate the VIPER ITM. The VIPER ITM correlation process had several schedule challenges, including the need to update the VIPER ITM and to correlate the thermal radiant heat enclosure (TRHE) used in the VIPER TVAC test after TVAC. *Veronica* enabled the VIPER team to meet its 22-week correlation schedule. This enabled the VIPER team to make their requirements verification deadline. The VIPER ITM used for verification employed only changes rolled in from the initial breakout model correlation. It achieved an RMS error of 7.4C|10C for hot | cold thermal balance and significantly reduced model errors compared to the uncorrelated ITM with 1.6 | 2.2 times more components reaching their error goals for hot | cold thermal balance.

Additionally, since there is very little public information about thermal model correlation times for real systems, this paper presented a survey of model correlate time and model complexity. The survey included 27 models, with 11 from VIPER and the VIPER ITM breakout models. The survey shows a general trend of longer manual model correlation times for larger, more complex models.

ACKNOWLEDGMENTS

We would like to thank Steven Rickman, Stephanie Mauro, and Kimberly Martin for helping with the model correlation time survey. We would also like to thank Jennifer Miller, Kaitlin Liles, Giuseppe Cataldo, William Birmingham, Savanna Lyles, Stephanie Babiak, Rezwanur Rahman, and Erik Stalcup for providing inputs to the survey.

[7] A local optimum would be a point in the search where the model error dips down but is not the point of lowest error (i.e. a valley).

REFERENCES

[1] "Ch 19. Thermal Testing," in *Spacecraft Thermal Control Handbook 2nd Ed.* , The Aerospace Corporation, 2002.

[2] NASA Passive Thermal Technical Discipline Team (TDT), Editors Kaitlin Liles and Ruth Amundsen, "NASA Passive Thermal Control Engineering Guidebook V4.0," NASA Engineering and Safety Center (NESC), 2023.

[3] R. a. S. Division, "Space Engineering, Thermal Control General Requirements ECSS-E-ST-31C," ESA , 2008.

[4] D. Hengeveld and J. Moulton, "Advanced Thermal Model Correlation Using Reduced-Order Models," in *ICES*, 2021.

[5] L. Maricic, "SWOT Thermal Model Correlation," in *TFAWS*, 2022.

[6] I. Torralbo, I. Perez-Grande, A. Sanz-Andres and J. Piqueras, "Correlation of Spacecraft Thermal Mathematical Models to Reference Data," *Acta Astronautica,* no. 144, pp. 305-319, 2018.

[7] I. Torralbo, J. Piqueras, I. Pérez-Grande and A. Sanz-Andrés, "A New Method to Correlate Thermal Mathematical Models of Space Instruments and Payloads," in *EUCASS*, 2019.

[8] J. Klement, E. Anglada and I. Garmendia, "Advances in Automatic Thermal Model to Test Correlation in Space Industry," in *ICES*, 2016.

[9] "5.10 Test Data Calibration Methods," in *TD Suite Manual for Thermal Desktop, TD Direct, and SINDA/FLUINT Version 6.3*, C&R Technologies, 2022.

[10] B. Frey, T. Trinoga, Hoppe and W. Ebelin, "Development of an Automated Thermal Model Correlation Method and Tool," in *ICES*, 2015.

[11] G. Cataldo, M. Niedner, D. Fixten and S. Moseley, "Model-Based Thermal System Design Optimization for the James Webb Space Telescope," *Journal of Astronomical Telescopes, Instruments, and Systems,* vol. 3(4) , 2017.

[12] "5.0 Advanced Design Models, TD Suite Manual V6.3," C&R Technologies, 2022.

[13] J. Turk, E. Stewart, T. Page, E. Medichi and J. Otero, "Volatiles Investigating Polar Exploration Rover (VIPER) System Integrated Thermal Vacuum Test," in *TFAWS*, 2025.

[14] S. Lyles, "Thermal Vacuum Testing Strategy and Thermal Desktop Model Correlation for the Moon to Mars Planetary Autonomous Construction Technologies (MMPACT) Robotic Terrestrial Arm," in *TFAWS*, Cleveland, 2024 .

[15] J. Miller, K. Singh, K. Novak and J. Lyra, "Mars 2020 System Thermal Vacuum (STV) Test Implementation and Results," in *ICES*, St. Paul, 2022.

[16] R. Amundsen, W. Davis, K. Liles and S. McLeod, "Correlation of the SAGE III on ISS Thermal Models in Thermal Desktop," in *ICES*, Charleston, 2017.

[17] A. Nijenhuis, H. Brouwer, M. Jonsson, E. Bloem, G. van Donk, B. Lamers, A. Pauw and R. van Benthem, "Thermal Analysis and Verification of CubeSat Designs with ESATAN-TMS," in *ICES*, 2021.

[18] J.-S. Kim, S. Lee, H.-K. Kim and H.-D. Kim, "Thermal Model Correlation of SNIPE Sattelite Using Genetic-Algorithm-Based Multi-Objective Optimization ethod," *Journal of Spacecraft and Rockets,* vol. 60, no. 4, 2023.

[19] J.-F. Ruel, J.-F. Labrecque-Piedboeuf, J. Newman, D. Mishkinis and G. Wang, "Thermal Design and TVAC Test Correlation of a Lunar Rover Prototype," in *TFAWS*, 2020.

[20] H. Tanaka and H. Nagai, "Thermal Surrogate Model for Spacecraft Systems Using Physics-Informed Machine Learning With Pod Data Reduction," *International Journal of Heat and Mass Transfer,* 2023.

[21] J. Arlanzón, F. Beltrán, M. Pujades, S. Vey and P. Hager, "Thermal Balance Test and Thermal Model Correlation of MetOp-SG ICI Instrument," in *ICES*, 2020.

[22] R. Amundsen, W. Davis, K. Liles and S. McLeod, "Correlation of the SAGE III on ISS Thermal Models in Thermal Desktop," in *ICES*, 2017.

[23] E. Stalcup, "Thermal Modeling and Correlation of the Space Enviornments Complex VAcuum Chamber and Cryoshroud," in *TFAWS*, 2018.